SACLANT UNDERSEA
RESEARCH CENTRE

MEMORANDUM

Interface-wave propagation studies: An example of seismo-acoustic propagation in non-homogeneous materials

M. Snoek

January 1990

Page count for SM-229
(excluding covers)

Pages	Total
i–vi	6
1–33	33
	39

SACLANT Undersea Research Centre
Viale San Bartolomeo 400
19026 San Bartolomeo (SP), Italy

tel: 0187 540 111
telex: 271148 SACENT I

NORTH ATLANTIC TREATY ORGANIZATION

Saclantcen SM-229

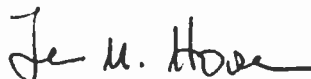# Interface-wave propagation studies: An example of seismo-acoustic propagation in non-homogeneous materials

M. Snoek

The content of this document pertains to work performed under Project 12 of the SACLANTCEN Programme of Work. The document has been approved for release by The Director, SACLANTCEN.

Issued by:
Underwater Research Division

J.M. Hovem
Division Chief

intentionally blank page

Sᴀᴄʟᴀɴᴛᴄᴇɴ SM-229

**Interface-wave propagation studies:
An example of seismo-acoustic
propagation in non-homogeneous
materials**

M. Snoek

Executive Summary: Important parts of NATO's operational areas are located on continental shelves. Sonar performance in these areas is strongly influenced by the physical properties of the seafloor and the coupling of acoustic waves in the water to seismic waves in the seafloor. An understanding of these interaction processes and of the physical properties of the seafloor material (mainly compressional and shear wave velocities, attenuation, and density) is essential for improved modelling and prediction of propagation loss in shallow water.

Interface waves are a special class of seismic waves that can be used as a diagnostic tool to probe the seafloor, particularly for the measurement of the shear wave velocity as a function of depth. This study addresses the experimental problems involved with the generation and propagation of these waves.

Ocean bottom seismometers recorded interface-wave propagation data received from explosive charges fired at the seabed at various ranges and bearings. Subsequent analysis revealed that there was a significant propagation variability in the sediments as a function of ranges, azimuth and depth that may be explained by seabottom material inhomogeneities.

Future experiments will have to be performed with higher spatial resolution of interface-wave data and a better coverage of high-resolution seismic survey data, complemented by sediment cores and in situ acoustic measurements.

intentionally blank page

SACLANTCEN SM-229

Interface-wave propagation studies: An example of seismo-acoustic propagation in non-homogeneous materials

M. Snoek

Abstract: This study addresses the problem relating to the interaction processes of the seismo-acoustic wavefield with the seafloor and sub-seafloor. Particular attention is devoted to an understanding and an explanation of the experimental problems involved with the generation, propagation and recording of interface waves. These seismic waves propagate at very low frequencies (2–20 Hz) and are further characterized by being polarized in the source/receiver plane (sagittal plane). It is shown that the propagation of these waves is very sensitive to material inhomogeneities. This fact, however, allows one to estimate material characteristics from propagation variations. Triaxial ocean bottom seismometers (OBS) are used to study these phenomena in situ.

The results of this experiment are given and the effects of material parameters on seismic propagation are demonstrated. The SACLANTCEN SAFARI code was used to model the dispersion behaviour of the interface waves. The results of the calculations are discussed.

Keywords: attenuation ○ bottom characteristics ○ compressional velocity ○ interface-wave propagation ○ ocean bottom seismometer ○ seabed characteristics ○ seismo-acoustic propagation ○ shear wave velocity

Contents

1

Introduction

About 60% of the experiments previously undertaken by SACLANTCEN to study interface/surface wave propagation failed or produced the results that were not interpretable in this direction. This extremely important observation demands a more detailed investigation into the causes of this behaviour. An interesting and intriguing fact of past experiments was the unpredictibility of the existence of interface waves in environments where seafloor material was expected to support interface wave propagation. Since we always deploy the same instruments and configurations and we use the same procedures to generate seismo-acoustic energy, the problem must be found in the propagation medium itself, i.e. the layer geometry and/or the elastic parameter of the propagation medium. In two seismo-acoustic experiments where energy was generated along linear profiles, the interface wavetrain could only be measured at one point (no indication of this wavetrain was found at lower or higher ranges). In a different region the interface wavetrain was clearly seen and recorded for a given c.w. source, but under the same experimental conditions a shift of the frequency by tenths of a hertz resulted in the disappearance of the interface wavetrain. Another surprising observation was that when the frequency content of the source was maintained but the azimuth of the track was changed, the interface signal was not observed.

Analysis of surface wave propagation on the shelf off SE Scotland recorded by the seismic LOWNET array (Crampin et al., 1970) showed that the seismic response was highly variable, although the epicentral area of the explosions was only small (~ 2 km^2). The absence of surface waves on some of the sensors was explained to be a result of interaction with structural features in the propagation medium, i.e. to variations in sediment thicknesses (MacBeth and Burton, 1988).

These observations as well as the phenomena described above lead to the conclusion that we are dealing with a very finely tuned system that is extremely dependent on the environmental parameters. It appears that source frequency, depth, geometry, interface roughness, layer heterogeneity and thickness play important roles in the successful propagation of surface waves and particularly interface waves.

To interpret the phenomena observed in the field, we have to understand the physics involved in the signal transmission from the source via the seabed to the sensors and to study the mechanism in areas with good ground-truth. The first part of the document briefly outlines what we think is relevant to understand the problem; the

second part presents results from an experiment designed to study interface-wave propagation in a known environment.

The seafloor represents a complicated liquid/solid lossy boundary, allowing the conversion of acoustic energy into seismic energy. An acoustic signal impinging on the seafloor generates a series of seismo-acoustic interaction patterns that depend on the frequency spectrum of the source, the angle of incidence, the attenuation of the involved propagation media as well as the surface structure (roughness) of the boundary. Interaction with the layered seabed creates similiar patterns; as a result we encounter wave conversions that create mixed-wave types, interferences, resonances and absorptions (Ganley and Kanasewich, 1980; Stoll et al., 1988). Since for most sediments we encounter a velocity increase with depth, we will observe upward refraction of seismic signals if layer thickness and/or the gradient support this. The effects of layered sediments on sound reflection has been reported earlier and is not the subject of this memorandum; here we want to investigate the processes leading to conversion into seismic waves. The seismic wavefield propagates in two modes, as body waves and as surface waves. Refracted waves, with the special case of the head waves, represent the first type, whereas Rayleigh waves, with the special case of the interface waves, represent the other type. An extensive review and a physico-mathematical background of the seismic interface-wave complex has been given by Rauch (1980, 1986) and some aspects on modelling have been presented by Jensen and Schmidt (1986). Despite the wealth of literature concerning the interface-wave complex, it can not be said that sufficient data are not available to establish correlations between environmental conditions and interface-wave propagation. A compilation of publications concerning this field and the main results is given in Table 1.

Defined by the boundary conditions (see Table 2), we talk of Stoneley waves or Scholte waves. Scholte waves are the more important ones for our studies, since they are confined at or near the seafloor, where the sensors are deployed.

In more consolidated seafloor sediments or in harder material one can encounter leaking Rayleigh waves (Phinney, 1961), also called pseudo-Rayleigh waves, if $c_{\text{Rayleigh}} > c_p$ in water, i.e. the Rayleigh wave travelling in the seafloor excites a radiating p-wave in the water.

Some of the significant characteristics of the interface waves are listed below; they are strictly valid only for an idealized environment, i.e. transversally and vertically isotropic lossless media:

- The Scholte wave speeds c_{Scholte} are always less than the sound speed c_p in water.

- The particle motion is confined to the plane that includes the source receiver direction and the vertical of the interface, also called the sagittal plane.

- Between the radial and vertical ground displacement there is a $\frac{1}{2}\pi$ phase shift.

- The hodographs display a regular elliptical shape.

- Interface wave energy decreases exponentially in the directions perpendicular to the interfaces.

- Significant penetration depth is about one wavelength.

Under realistic field conditions, i.e. lateral varying and/or layered media we will find:

- The interface wavetrain is dispersive.

- Scholte waves are strongly attenuated.

- Mode conversion due to complicated propagation geometry.

- The polarization plane will be rotated with respect to the sagittal plane due to anisotropy, inclined due to material inhomogeneities and finally tilted due to loss mechanism.

Table 1   *Previous interface-wave experiments and results (after Jensen and Schmidt, 1986)*

Investigators	Year	Water depth (m)	Bottom type	Centre freq. (Hz)	Measured atten. (dB/km)	Inferred shear speed (m/s)	Inferred shear atten. (dB/λ_s)
Bucker et al.	1964	1	sand	20	300	100	1.4
		20	sand	25	200	195	1.4
Davies	1965	4410		6		50–190	
Herron et al.	1968	5	silt	5		40–115	
Hamilton et al.	1970	390	silt			100	
		985	silt			90	
Schirmer	1980	130	sand	4.5	7	120	0.2
McDaniel and Beebe	1980	32	sand	10		200	
Essen et al.	1981	1	silt	4		75–250	
Tuthill et al.	1981	7	mud	4.5		25–50	
Whitmarsh and Lilwall	1982	5260		4.5		25–170	
Holt et al.	1983		sand	35	600	135–195	2.3
Brocher et al.	1983	67	sand	5	0.43	260	0.02
Schmalfeldt and Rauch	1983	20		3	10	100	0.3
		30		3	2	150	0.1
Möller	1983	30	sand	5.5		200–400	
Staal and Chapman	1986	150	granite	4		1200	
Sauter et al.	1986	3800		2		35–100	
Snoek et al.	1986	105	silt	4		65–360	
Schmalfeldt and Ali	1987	28	silt	2		20–105	
Snoek and Rauch	1987	17	silt	4		98–150	

Although a general qualitative picture of interface/surface wave propagation emerges from our own experiments and as survey of the literature, it becomes clear, that, due to the complexity of the processes regarding wave generation, transmission and

Table 2 *Classification of interface waves (after Phinney, 1961)*

Class of interface	Type of free interface wave
Vacuum/	Rayleigh wave
Solid (c_p', c_s')	$c_{Rayleigh}' = n'c_s'$
	$0.873 < n' < 0.957$
Liquid (c_p)/	Scholte wave
Solid (c_p', c_s')	$c_{Scholte} \leq \min\{c_p, c_s'\}$
Solid (c_p, c_s)/	Stoneley wave
Solid (c_p', c_s')	$\max\{c_{Rayleigh}, c_{Rayleigh}'\} < c_{Stoneley} < \min\{c_s, c_s'\}$

detection, a more systematical multiparameter survey has to be performed; we need a good description of the source, the geoacoustical parameters of the seafloor and seabed, and an outline of the geological facies conditions and of seismic propagation. The objective of this paper was to indicate the problems involved generating and recording interface waves and analyse the data obtained from the experiment conducted on the Ligurian Shelf. Finally, we want to demonstrate the variance of the propagation medium, i.e. the influence of the environmental characteristics on the propagation of interface waves.

Special attention in the experiment described in this memorandum was devoted to the generation and observation of boundary waves guided in the acoustically most relevant interfaces, complemented by the collection of cores as well as a high-resolution seismic survey.

An analysis of compressional waves is included to help describe the material properties of the deeper layers.

2

Experiment

Experimental set-up   The basic tool of the interface wave experiments is the ocean bottom seismometer (OBS) developed at SACLANTCEN in 1978. The sensor pack, which also contains the preamplifiers and A/D converters, is linked by cable to a surface buoy that transmits the multiplexed signals to a receiver station. The seismic sensors consist of 3 TELEDYN S-500 seismometers arranged triaxially. Every unit is also equipped with a thermistor to measure the water temperature and sensors for monitoring the inclination and azimuth of the geophone station. An omnidirectional hydrophone is mounted outside the sensor pack. A detailed report on all relevant technical aspects has been given by Barbagelata et al. (1982).

The interface wave experiment was divided into two parts. On the first leg (pre-site survey) we operated with only one OBS that was connected to a large permanently moored buoy and telemetrically linked to our land base. In addition to an initial seismic interface-wave experiment designed to gain some idea of propagation characteristics, we ran high-resolution seismic profiles to determine the core locations and delineate seafloor and sub-seafloor boundaries. The second leg, and the main experimental phase, was conducted with two ships, the research of vessel *Maria Paolina G.* (MPG) and the T-boat *Manning* (Fig. 1). In order to avoid redeployment and time delays, we designed the configuration of sensors to enable us to perform seafloor and sub-seafloor propagation studies with high spatial resolution. The adoption of standard procedures in seismology to locate earthquakes and (nuclear) explosions with the help of seismic arrays lead to the installation of a tripartite network of OBS on the seafloor. Applying principles derived from land seismic studies which state that the maximum sensor separation, respective to the array size (diameter), should correspond to at least 1/10 of the observed distance, we placed the OBS $\sim$ 500 m apart (Fig. 2) in order to study events 5 km away. On the other hand, it was to be expected that this would be outside the coherence length for interface waves, since we are looking at signals with a wavelength of $\lambda \approx 25 \pm 10$ m.

The OBS were linked to small telemetric buoys that transmitted the signals to the receiving ship MPG. In comparison with the first leg, the signal-to-noise ratio was not good because of changes in the system (lighter anchor, smaller surface buoy) and a high sea-state. Seismic charges fired from the T-boat were attached to a weight, lowered to the seafloor on a cable and detonated electrically. Distances between the ships, the array and the reference buoy were continuously monitored by radar, while positions were taken with LORAN C. Since all positions remained static at the time of firing a charge, we have an adequate knowledge of the geometry at each shot
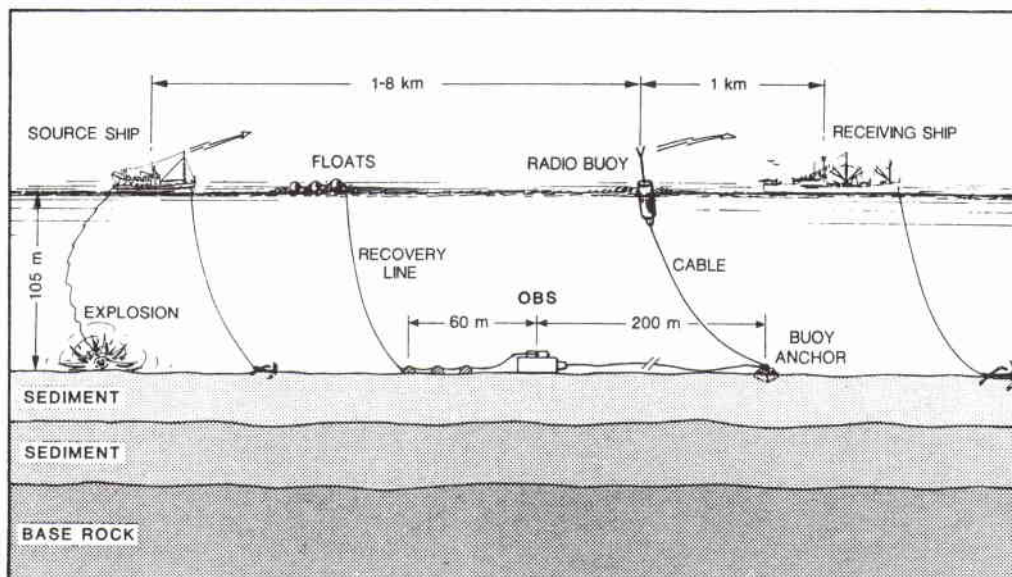
Figure 1 *Experimental set-up.*

that enables us to estimate the errors involved (see below). Experiments were done along seven profiles with the origin at the array (Fig. 2). To obtain a reasonable azimuthal coverage, more profiles would have been necessary, but under the given weather conditions the achieved coverage was quite good and represents fairly well the typical propagation conditions encountered on shelf areas.

Eleven sediment cores were collected with a 4-m gravity corer (Fig. 3).

Seismic sources For the seismic propagation experiment, explosive charges were fired on the seafloor. Although only $\sim$ 3–5% of the total energy of explosive charges fired in the waterbody is converted into seismic energy, a reasonable energy source level at the low-frequency range 2–20 Hz can be obtained. It is, however, convenient for our purpose to place the source as close as possible to the seabed to maximise energy conversion. We used small charges (180–1440 g) fired on the seafloor, allowing energy to be generated at the same datum plane the sensors are placed on. It further provides sufficient energy for the horizontal or shear component, which is required for the generation of seismic surface (interface) waves. The energy distribution in the time and frequency domain of a recorded signal generated by an explosive charge near the OBS (550 m) can be seen in Figs. 4a and b. The signal in the time domain is slightly clipped for the direct water wave on this plot; the interface wavelet starts at 5 s and can be seen to $\sim$ 14 s. In all, 97 shots were fired on seven profiles.

Inherent problems in the use of geophones To present quantitative results of interface wave propagation, one has to investigate all aspects of the propagating wavefield. The conversion processes of acoustic into seismic energy, the coupling of the

– 6 –
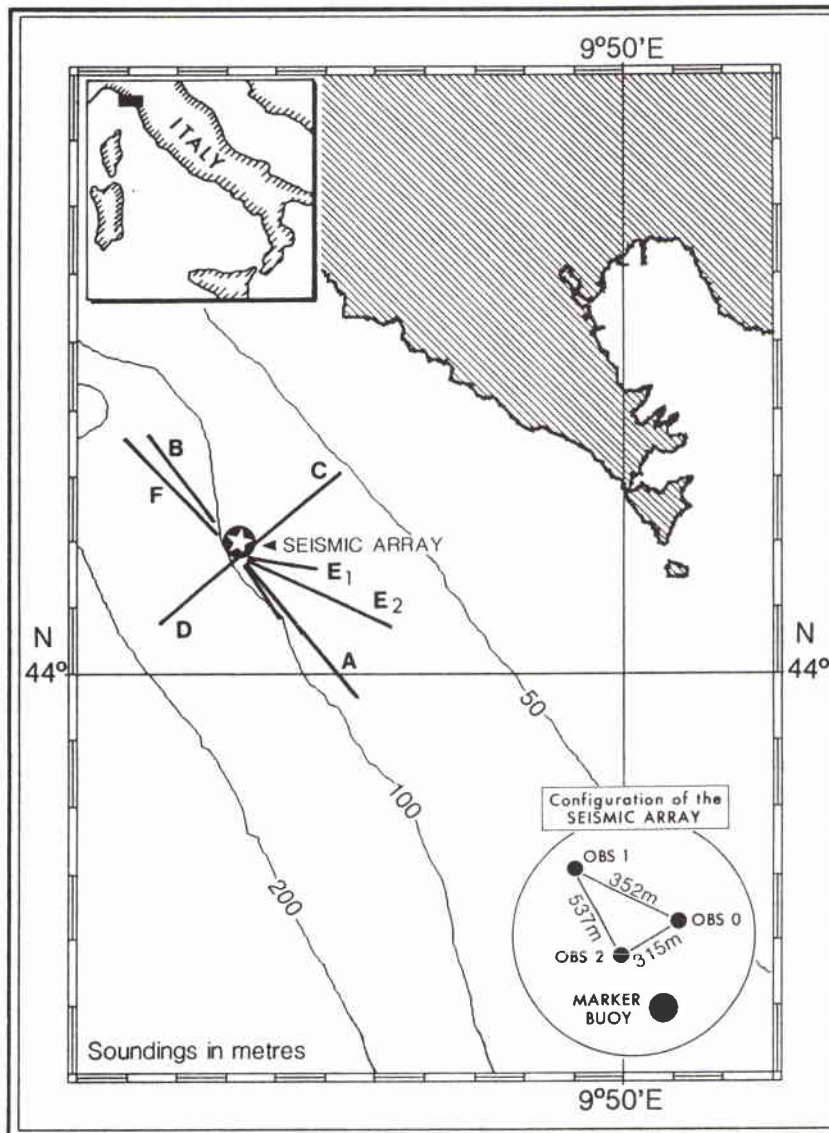
Figure 2 *Experimental tools and layout of the OBS array.*

waves propagating in the bottom to the sensors and the coupling of the sensors to the ground have to be understood fully in their physical context. The coupling phenomenon has been studied and is understood to some extent; results have been published in reports Lopez Island, OBSCAL and associated papers (Sutton et al., 1981a,b; Snoek et al., 1982; Trehu, 1985; Snoek and Herber, 1987; Sutton and Duennebier, 1988). However, the complete theory of the system's behaviour in its vertical and especially in its horizontal, components has not yet been presented. Since the horizontal components are of particular interest to us in order to analyse the motion plane, corresponding to the sagittal plane under ideal propagation conditions
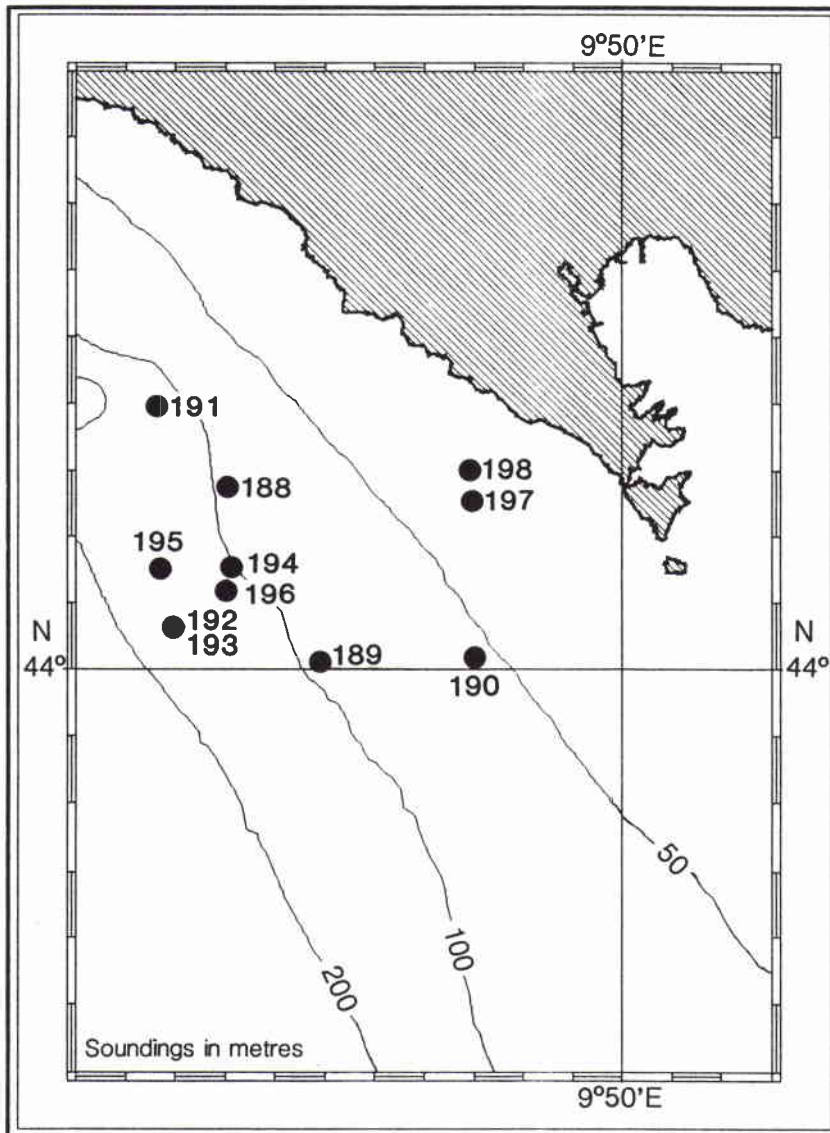
Figure 3 *Position of cores.*

(i.e. isotropic propagation medium), an adequate formulation of the full solution of coupling is required. This will be of special interest and importance when using sensors sitting on very soft material, penetrating into the mudline. A more important situation concerns sensors buried in man-made holes, since in this case the normal propagation/coupling material has been disturbed and there is little control over the actual coupling of the sensors to the propagation medium.

In the frequency domain, the total response S of an OBS can be described in very
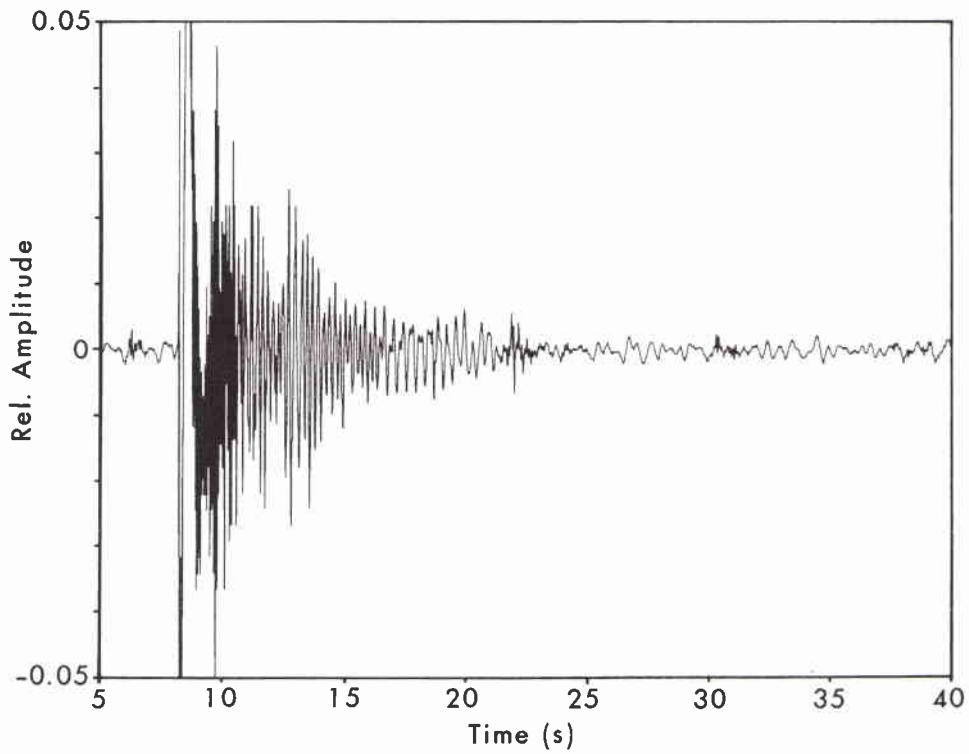
Figure 4a   *Bottom charge fired at 550 m from OBS.*

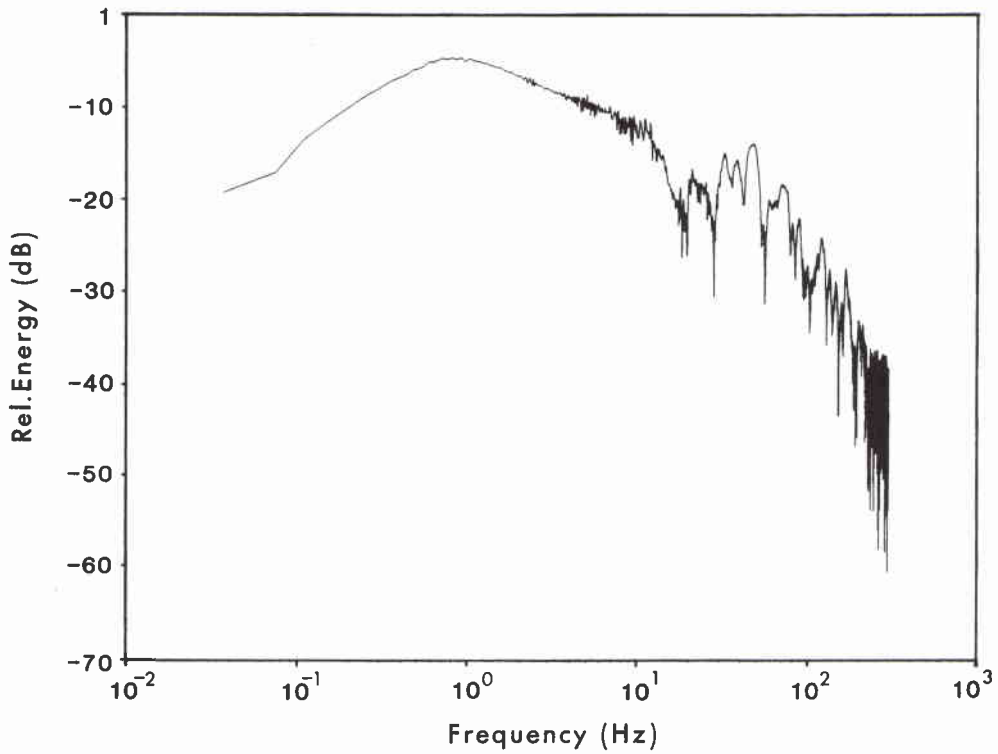**Figure 4b**   *Frequency spectrum of a bottom charge fired at range of 550 m.*

general terms as the product

$$S = S_1(\omega)\, S_2(\omega)\, S_3(\omega)\, S_4(\omega),$$

where $S_1(\omega)$ is the coupling of the OBS base to ground and water, $S_2(\omega)$ the coupling between the OBS casing and seismometer, $S_3(\omega)$ the response of the seismometer and $S_4(\omega)$ the source function.

For seismic work we have to know the effects of coupling an OBS to the ground, since the assumption that the transducer case motion and the free undisturbed soil particle motion are identical can not be supported. What we really want to measure is the free wavefield arriving at the sensors. However, this is generally not possible, since the transducer draws energy from the wavefield due to inertia effects and returns it with a phase difference; hence the data are no longer representing the free field. What can be done, however, is to design the sensors in a way that minimizes these effects. Because the sensor and the ground form a mechanical oscillating system with the coupling material being the variable, a distortion of the radiated original signal due to resonance phenomena may occur. Since in most cases we can not select the sites and hence the type of seafloor material, we have to choose the correct dimensions of the sensor unit so that resonance frequencies can be shifted out of the actual frequency range of interest.

We are using hodographs (particle velocity plots) for the discrimination of wave types and for direction analysis. To what extent the coupling complex distorts the particle motion and thus biases the directivity resolution of the sensorpack should be investigated. For a quantitative description that attempts to establish criteria concerning this problem, one has to be careful in selecting both the instruments and the experimental set-up. This has to be done in an extremely controlled environment, which allows an analysis of the individual components of distortion. Since in field experiments we generally only observe effects integrated over the entire propagation path, it will be necessary to localise, identify and quantify sources of distortion. This will further show whether a reasonable compromise has been achieved with respect to minimizing the coupling effects for the SACLANTCEN OBS. Results from previous experiments suggest that the system generally performs reasonable well on silty and on sandy marine sediments. However, as mentioned above, we have had experiments with no results, some of which can possibly be explained by incorrect/insufficient coupling.

3

High-resolution seismics

To map the seafloor and sub-seafloor layering, a high-resolution seismic profiling system was used. We operated the UNIBOOM in the frequency range 1–10 kHz with an output power of 300 J. Signals were recorded with a 7-element hydrophone array with an element spacing of 40 cm. Both source and array were towed ∼ 30 m behind the T-boat with a horizontal spacing of ∼ 10 m. Towing speed was ∼ 4 kn, the lowest possible stable velocity for the T-boat. The resolution of this method was limited by the ship's minimum speed and array-induced flow noise.

Layer discrimination On 16 km of profiles run over the area (Fig. 5), we obtained sufficient penetration and resolution to discriminate the sediment layers down to the bedrock. This material, probably of calcareous origin, represents the last glacial erosional platform. It is evident from this survey (Figs. 6–8) that the environment is characterized by:

- Surface roughness (on profiles parallel and oblique to the coast).
- Wedging of sediment layers (on the profile parallel to the coast).
- Change of sedimentation types and thickness.
- Gravitational slides and crossbedding (on profiles oblique to the coast).

Surface roughness was caused by slumping of the younger topmost sediments as well as by erratic sediment accumulations. Slumping and sliding of sediments are caused by gravitational forces acting on sediments deposited on slopes. The erratic sedimentation is probably current induced.

Crossbedding features encountered in the top sediment layers are further indicators of modern sediment dynamics. Further characteristic of profile C, which is our principal profile since the water depth remains constant at ∼ 100 m and it lies in the main striking direction of the geological environment (NW–SE), are:

- The outcropping of the layers at the NW (left) end of the profile (Fig. 6).
- The bedrock marked by fracturing and a rough surface.

These features are the result of most recent geodynamical processes active in the shelf areas adjacent to the Tyrrhenian Sea (Damiani, 1970; Selli, 1973; Finetti and Morelli, 1973). After the last glacial period, when interface GS (Fig. 6) represented
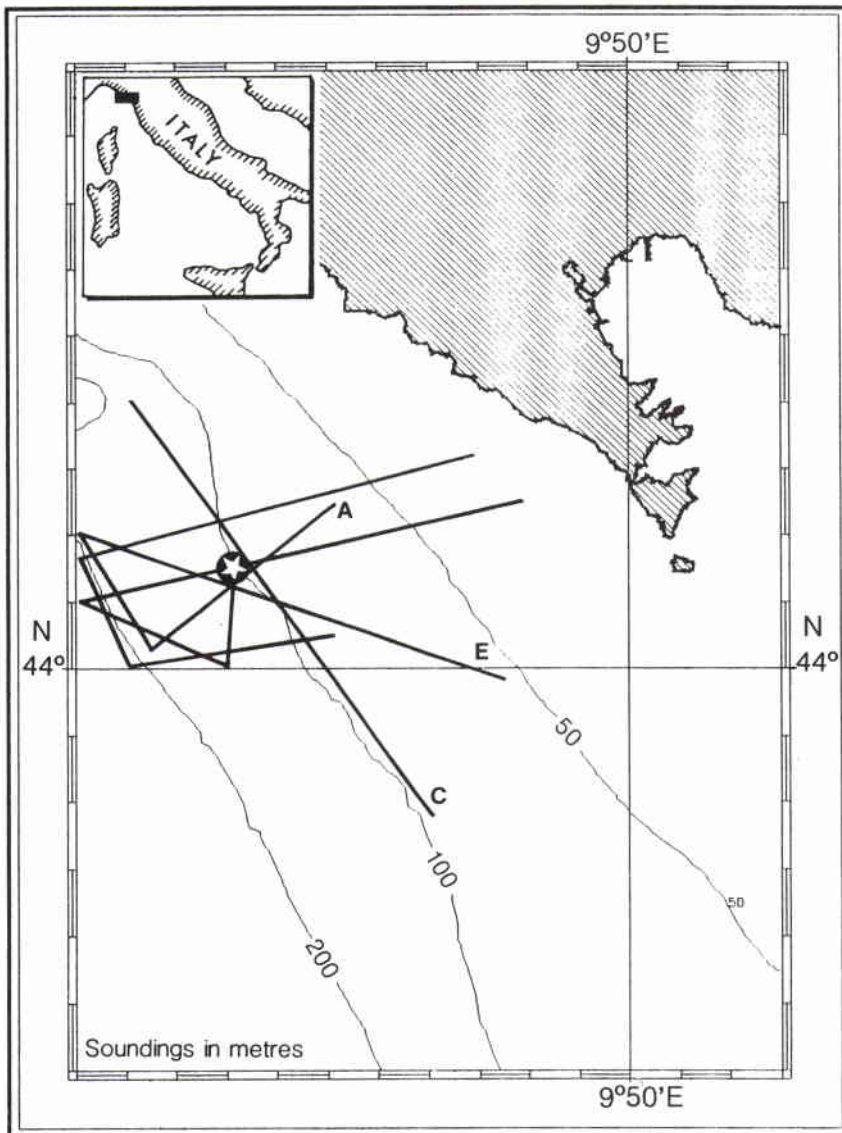
Figure 5 *Track chart of high-resolution seismic profiles (UNIBOOM).*

the surface and as such was exposed to glacial erosional processes, tectonic activity caused fracturing and differential vertical motions of the block, creating new erosional surfaces. This process can explain the wedge-like structures and the outcropping of the older layers as well as the angular unconformity of younger sediment layers. As sedimentation processes continued, this new surface was covered discordant with 4–5 m of sediments, from more sandy materials at depth to the present silty seafloor. It appears that in the SE part of the profile most recent activities resulted in erratic extraordinary sediment accumulation (Fig. 6). The geomorphic features are interpreted as very recent current-induced sediment accumulations. It
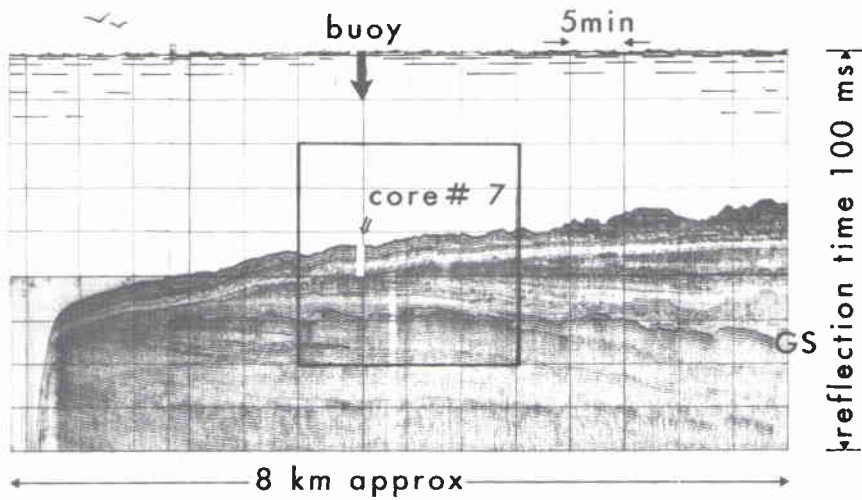
Figure 6 *Track C of high-resolution seismic profiles (UNIBOOM).*
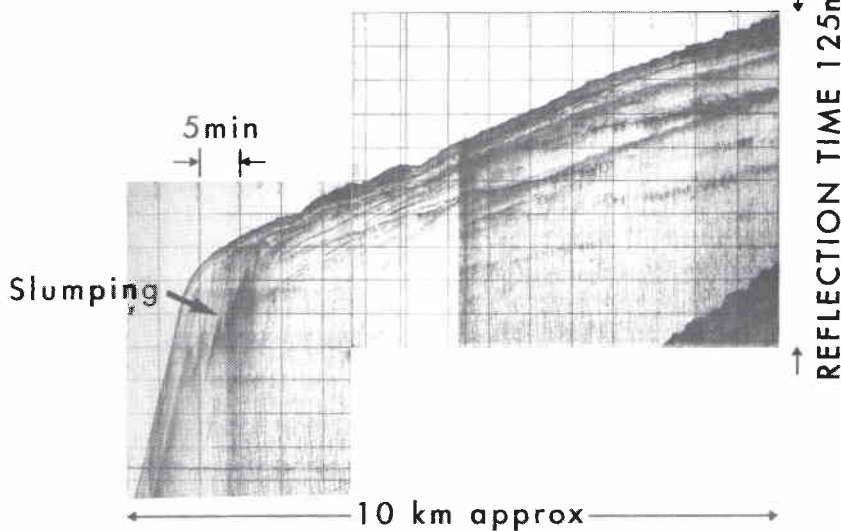
Figure 7 *Track E of high-resolution seismic profiles (UNIBOOM).*

cannot be ruled out, however, that they are of anthropomorphic origin (discharge area of port dredging activity).

The area of investigation certainly does not represent a simple system of lateral homogeneous layers, but depending on the azimuths of the profiles we encounter very different morphological regions. It is clear from this scenario, that it presents a difficult environment for the propagation of seismic waves in general, even more so for shear and interface waves.

Generalisation   The above described environment and shelf conditions are by no means unique, but are commonly found on continental shelfs and continental rises. Slope instabilities and anomalous sediment accumulations at river discharge areas as well as current-induced sedimentation add to the picture of a propagation envi-
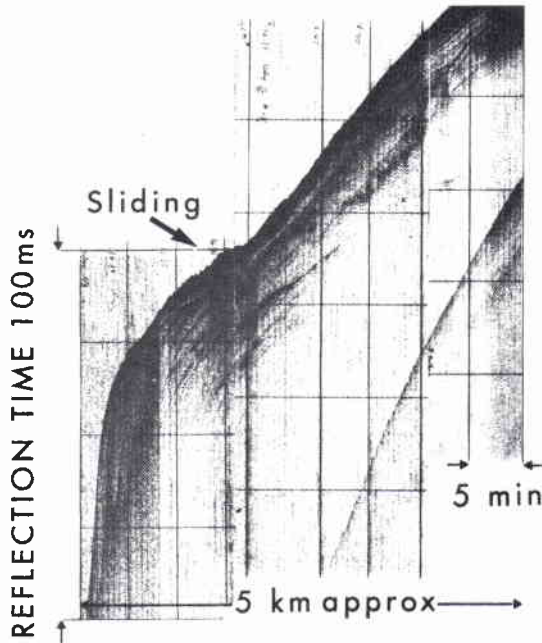
Figure 8 *Track A of high-resolution seismic profiles (UNIBOOM).*

ronment exposed to recent dynamical sedimentation processes. It can be said that the case of vertical and lateral variance represents the *normal* case of propagation media.

Structural elements of the seafloor and seabed, ranging from steep-angle layers acting as a propagation duct away from the surface, to rapid variations of sediment thicknesses and to such features as crossbedding and slumping as well as faulting, interfere with the generation and propagation of shear and interface waves. These effects, as well as rough surfaces of seafloor and sub-seafloor interfaces, will scatter seismic energy and reduce signal levels. It is easy to understand from this, that the propagation of energy over larger distances can be difficult and sometimes even impossible. The effects will be strongly variable in space, thus hindering reliable predictions of wave propagation.

The area we have chosen thus represents a realistic scenario showing most of the features indicated above.

4

Results of the seismic
interface wave experiment

Observations The two data sets available from the first and the second leg give a good impression of the quality of data as a function of weather and instrument configuration. It is clear that on the second leg of the experiment the conditions were much less favourable for the observation of interface wave propagation, partly due to the increased noise level induced to the seafloor from the rough sea (Akal et al., 1986), and partly because of the sea-state induced noise directly via the mechanical system. Whereas the first part of the experiment was performed at sea-states 0–2, the second part was conducted up to sea-state 6. The power spectral density of the ambient-noise levels at different OBS sensors for different sea-states are shown in Fig. 9. These spectral estimates were obtained by applying standard techniques to sections of 25 s over a 1–100-Hz frequency band and averaging the power spectral density levels over a 1-Hz bandwith.

The vertical geophone (*z*-component) and, in some cases the hydrophone gave the best results, indicating that the fundamental mode is the least disturbed or least attenuated mode of propagation (Figs. 10 and 11). It can further be taken as an indication that the *z*-component and the hydrophone are the least critical in their coupling to the propagation medium.

With the a priori knowledge of the propagation medium, it was predicted that good seismic results would be obtained in the first 2.5 km in the direction parallel to the coast, since the propagation path is formed by 'undisturbed' sediments of same thickness and facies conditions.

Seismic velocity data To determine the seismic velocities of compressional and interface waves along the profiles, two different approaches were followed:

- The standard seismic approach of stacking the data in time versus range plots was used to correlate the phase and group velocities.

- The method of dispersion analysis using the multiple filter technique (MFT) (Dziewonski et al., 1969) was used to obtain a plot of mode energy as a function of group velocity and frequency.

Compressional wave (p-wave) velocities were analysed only for profile C (the profile parallel to the coast), since on all other profiles sloping seafloor as well as sloping
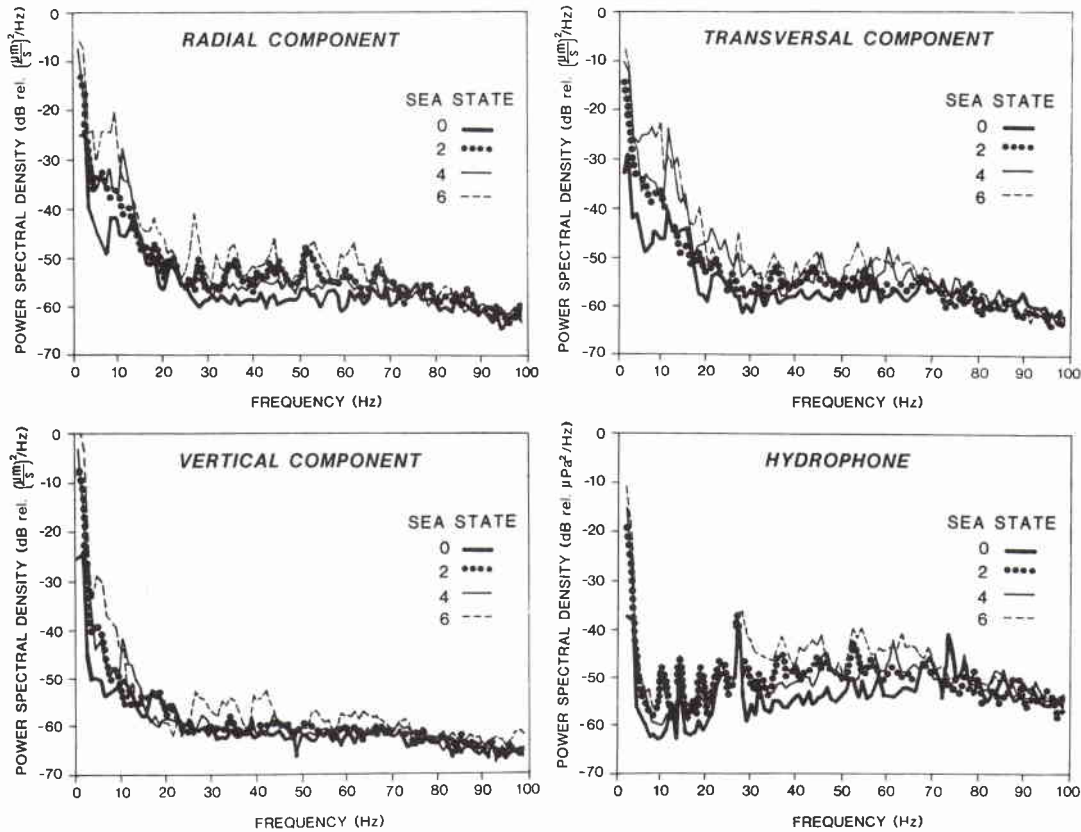
Figure 9 *Power spectral density levels of OBS recorded noise for different sea-states (after Akal et al., 1986).*

interfaces encountered will lead to dip-dependent apparent p-wave velocities. The correlated p-wave velocities from 1.6–3.1 km/s are generally in the expected range and are typical for this type of environment. All our profiles are split profiles, i.e. we only observe the seismic propagation in one direction; hence all velocities are apparent velocities. On profile C, however, the differences to real velocities are small, since the dip of layers can be neglected.

We have determined the group velocities by correlating the energy maxima of the envelope of the groups, the beginning of the wavetrain and the slow end of the wavetrain. This correlation method can only be applied with caution to group-velocity data, since individual modes are not always clearly separated and the wavetrains are highly dispersive. In the case of noisy data and in environments where we only encounter mixed-mode situations, this method will fail. The modal structure of the interface wavetrain will be a result of superpositions of modes generated in the seafloor, the sub-seafloor strata and at the structure irregularities. Lateral variance of the propagation medium will further create interferences, which will at best be difficult to correlate and interpret with standard seismic techniques. In applying this technique to our data we have nevertheless obtained a fairly reasonable agree-
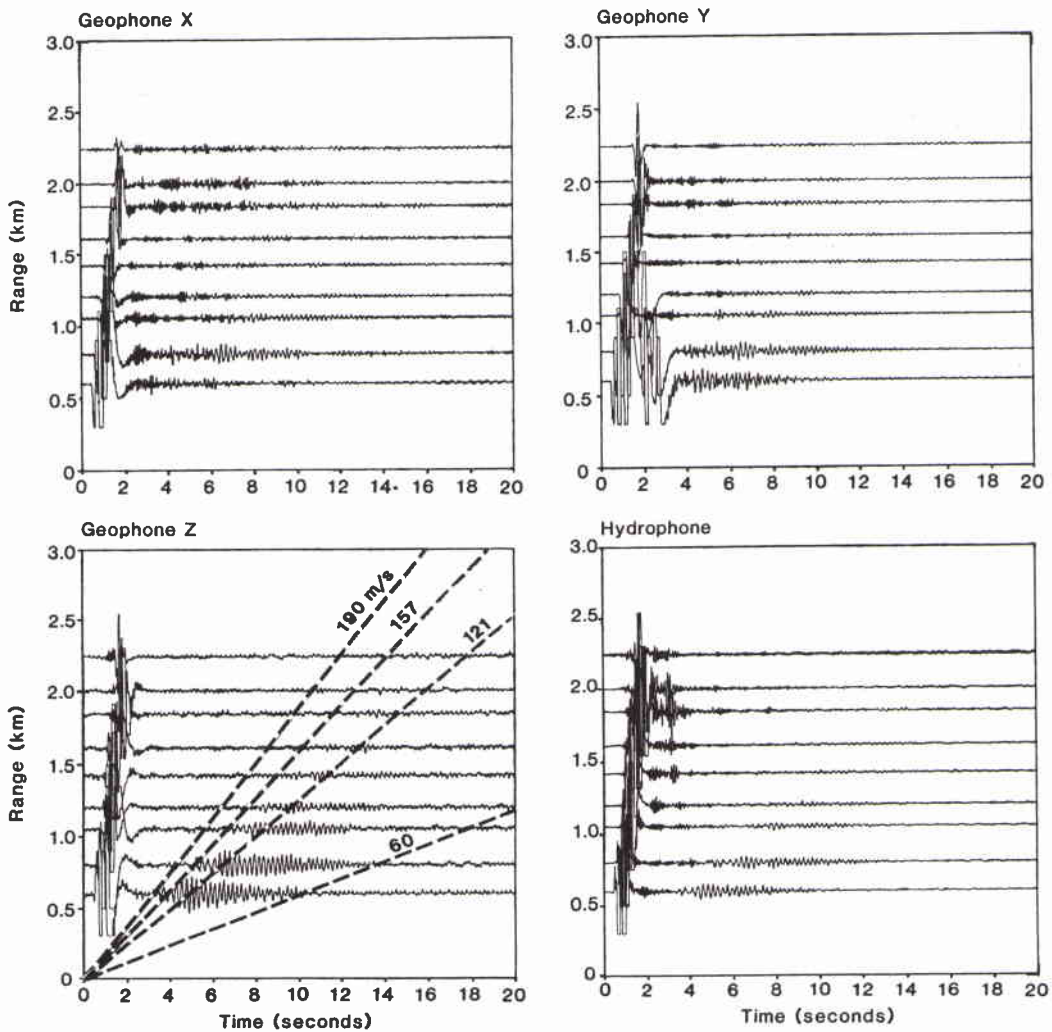
Figure 10 *Three component plus hydrophone recordings of an OBS on profile B.*

ment between the different profiles, with the exception of data for profile F. Results are compiled in Table 3. Data for profiles E_1, E_2 are not included, because weather conditions were extremely bad, resulting in a poor signal-to-noise ratio.

Since the MFT separates modes in the wavetrain, we have a more appropiate tool to determine mode velocities. The identification of the mode order is supported by analysing both, horizontal and vertical geophone data as well as by investigating the particle motion plots for that particular time window. The results of the MFT are displayed in a Gabor matrix, i.e. the display of the interface wave energy as a function of frequency and group velocity calculated for a given range. The velocities obtained with this method are in good agreement with results obtained from correlations as described earlier. The dispersion of the interface wavelet is strong; for the narrow frequency step from 4 to 6 Hz the group velocities decrease from

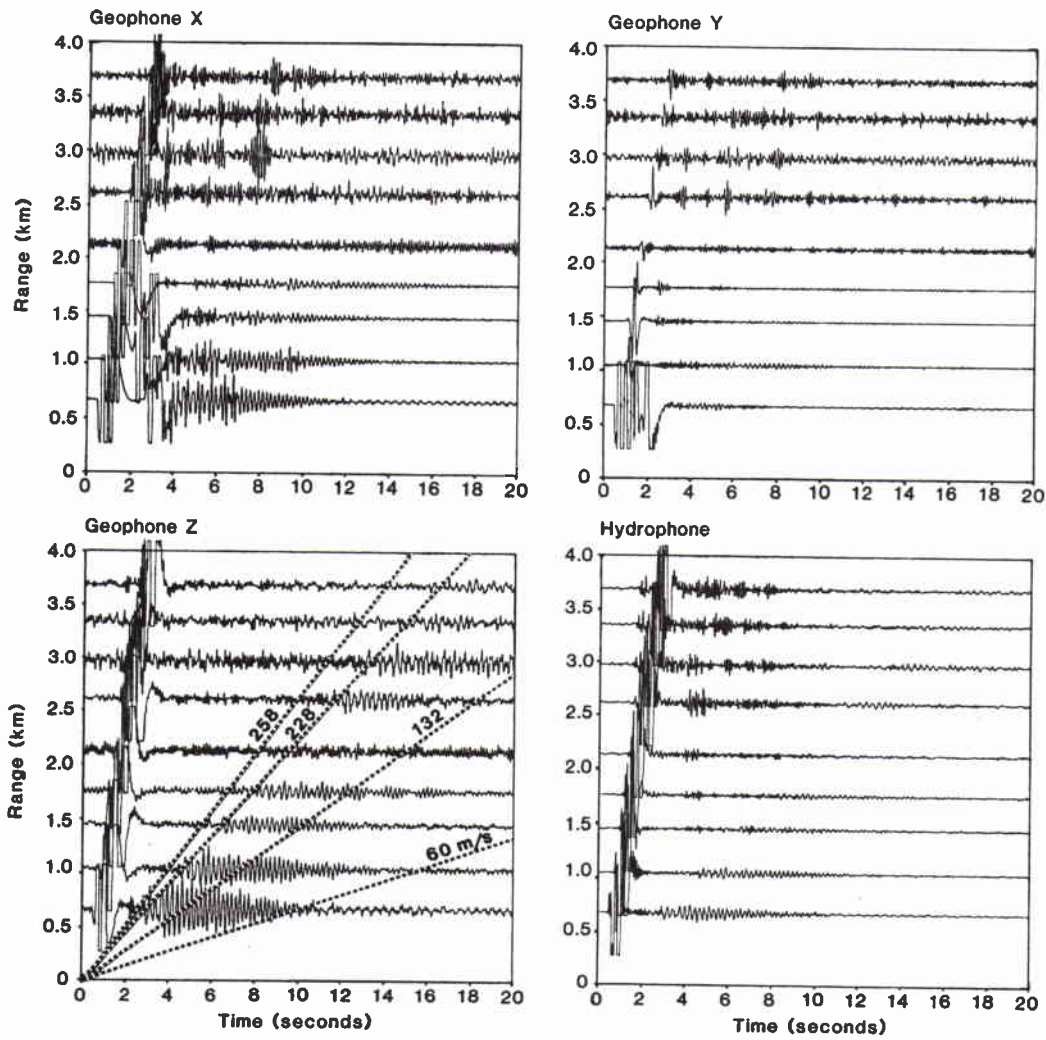**Figure 11** *Three component plus hydrophone recordings of an OBS on profile C.*

Table 3 *Interface wave mode velocities*

Profile	Azimuth (°)	Mode velocities (m/s)			
A	143	65	122	170	260
B	316	60	121	154	190
C	058	60	132	228	258
D	249	66	143	192	242
F	320	88	210	235	325

200 to 60 m/s with 40 m/s reached at $\sim$ 8 Hz. Below this velocity the dispersion curve is almost horizontal; i.e. there is no observed dispersion. This indicates the high stratification and/or gradient of the sediment cover. If we use the fact that the interface wave 'senses' down to about one wavelength, we can conclude that the material encountered between $\sim$ 5 m and $\sim$ 50 m has the high-velocity gradient mentioned above. The first 4–5 m have a fairly uniform consistency, which is in fact confirmed by core analysis data.

The MFT will clearly indicate the dependency of the modal structure of interface waves on transversal and lateral material inhomogeneities. The fast disappearance of a clearly defined modal structure with distance from the receivers (Fig. 12) is in fact indicating a complex mixed-mode environment.

In Table 3 all interface mode velocities obtained from standard correlation techniques were compiled as function of profile azimuths, showing a considerable variability for the higher modes.

Interface wave energy   Reliable results for the attenuation of interface wave energy can only be obtained by analysing the individual modes of the wavetrain. This requires however, that modes of different order be identified and clearly separated. Since in the area investigated the propagation media supported the creation of a multi-mode interface wavelet, only the energy of the entire interface wavetrain could be analysed and no absolute attenuation calculations were performed.

Spectral energy for predominant frequencies 4–6 Hz and 8–9 Hz was calculated and displayed as function of range (Fig. 13). Two remarkable features show up:

- The trends observed, i.e. the variation of interface wave energy with azimuth, are not consistent for different frequencies.

- An energy minimum for the 8–9 Hz frequency range on profile F is followed by an increase of energy by $\sim$ 18 dB from profile F $\rightarrow$ B for the range $x = 1130$ m, whereas we find a maximum of energy for the 4–5 Hz range on profile F followed by a decrease of energy of the same magnitude from F $\rightarrow$ B.

If we take into account that penetration depth is a function of frequency (i.e. low-frequency energy penetrates deeper than high-frequency energy), our results indicate that the upper sediments are more homogeneous than the deeper strata. This means we have less variation in energy levels for 'higher' frequencies and a more complicated and incoherent pattern for the 'lower' frequencies. This picture is consistent with results obtained from the high-resolution seismics on profile C, where for the first 1500 m we find a uniform layer of 4–6 m thick unconsolidated sediments, overlaying a disturbed sub-seafloor referred to as bedrock (acoustic basement). It should be pointed out that our results are based on single events. The assumption that energy generation is stable and reproduceable does probably not hold for this experimental area. Encountering different geomorphological regions within our experimental area
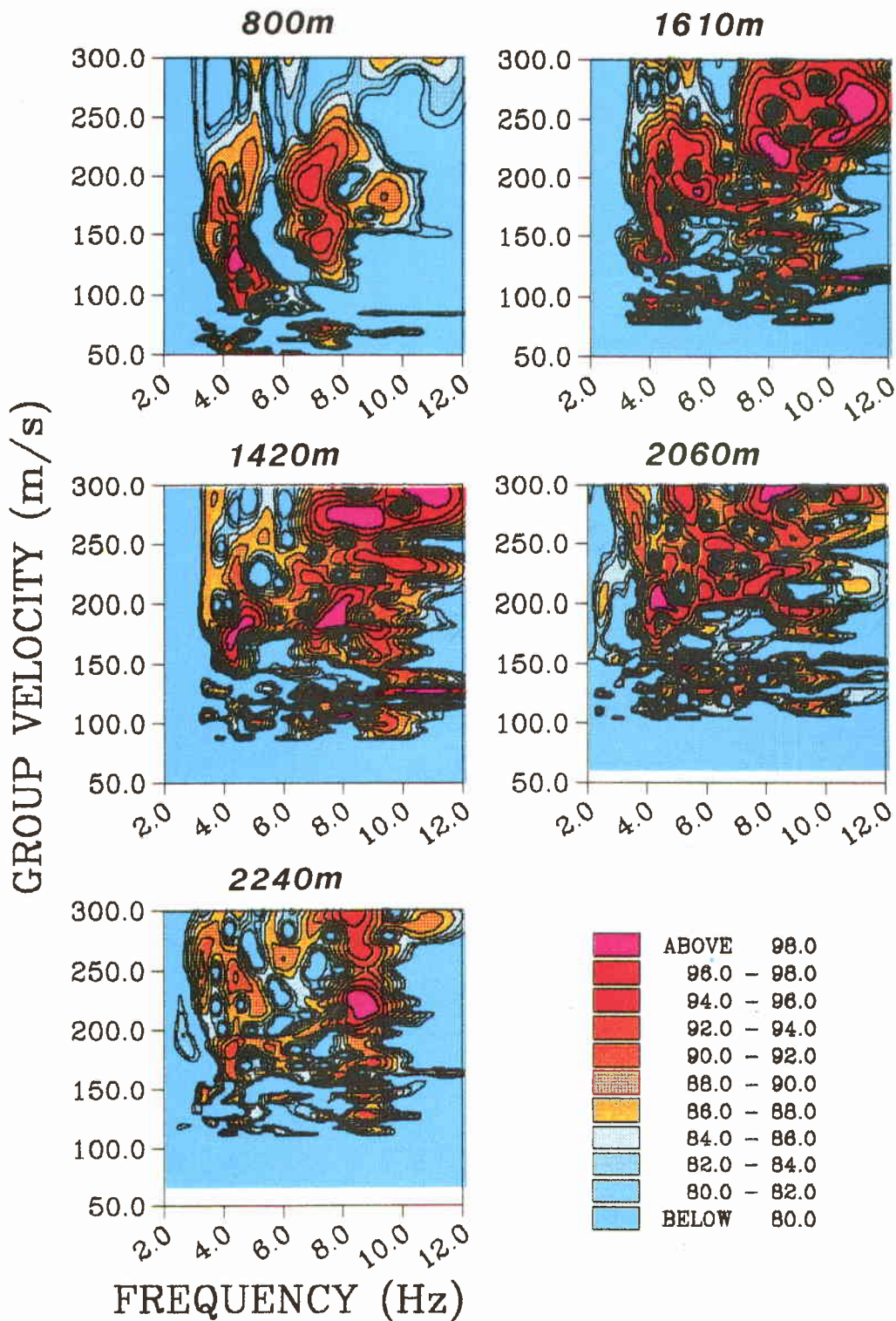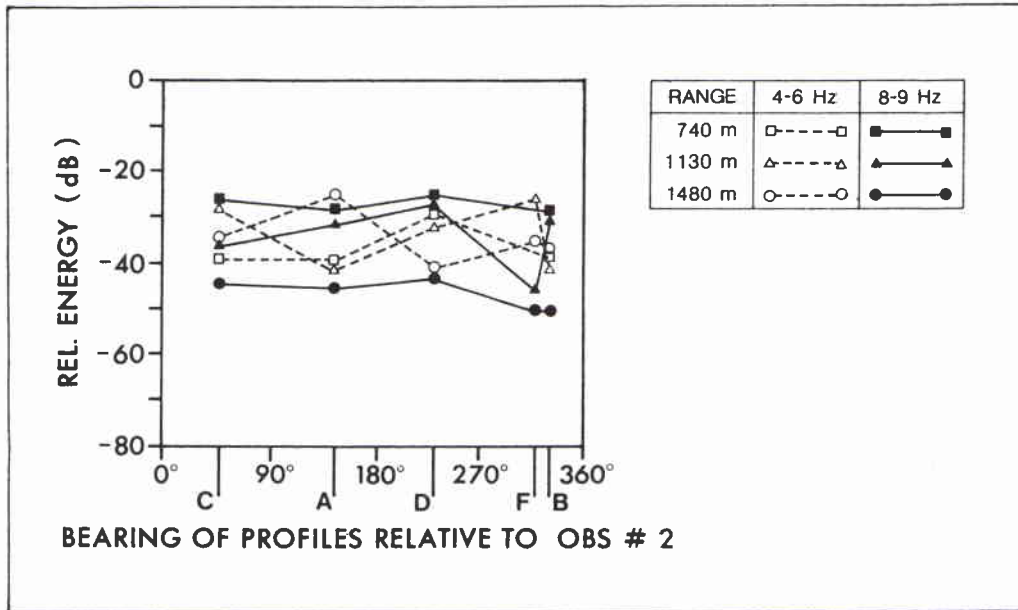
Figure 12 *Interface wave energy displayed in Gabor matrices for different ranges.*

-

Figure 13 *Interface wave energy as a function of profile bearing, frequency and range calculated for standard bottom charges (180 g).*

will have an impact on energy generation and energy coupling; thus any statements made will have to be taken with some caution. However, the fact that anomalies observed in travel times (i.e. here interface wave velocities) as well as in energy distribution show up for the same profiles indicates that we encounter changes in the propagation medium, i.e. material hetereogeneity. It remains impossible, however, to infer generally valid propagation pattern from these data, since the variability of experimental conditions was too high.

Error estimation All experimental data have system inherent uncertainties and/or error bounds. The errors involve the precision of the source position (position of the ship at the time of the shot, position of charge on the ground), the reading errors in the time series, the accuracy of the sound velocity in water as well as time synchronisation errors. In general, with carefully planned experiments and with all involved systems working properly, these errors can be minimized. All range and time information t_0 was based on the ship's navigational systems (SATNAV, LORAN C and radar) controlled by using the direct waterborne path of the shock wave recorded with the OBS's hydrophone. Working near to the coast we were fortunate to be able to use a permanent navy buoy as an instrument platform on the first leg and as a reference point on the second leg. The position of this buoy was known to an accuracy of ±20 m, verified several times in that year-by-test trials. This eliminates the problem of absolute and relative positions, since we were permanently able to correlate all positions obtained from the different systems with the position of the reference buoy. All our range information was referenced to this buoy, which was equipped with a large radar reflector. The LORAN C system

worked with an accuracy of ± 20 m (*relative positions*); the precision of the radar depended on the sea-state. Since the position of the charge was taken when it hit the seafloor (during the shooting procedure the ship was moored), we can assume that the errors in estimating positions were within 20 m at times of low currents to 50 m at times of higher currents at shallower depths; corresponding values in the deeper water were up to 50 and 150 m, respectively. This means that the best estimate for the charge position lies $\sim$ 20 m, the worst $\sim$ 170 m. For direct waterborne path readings this means ± 113 ms in the bad case and ± 13 ms in the best case. If, however, we take the largest range uncertainties and apply them to the slow travelling interface waves, we can expect timing errors of the magnitude of 500 ms up to 1000 ms. This is imprecise even for qualitative considerations. We can check the quality of our position by correlating the different phases using the conventional seismic stacking of traces in the time-range plots. With the given velocity c_p for the water wave all time series can be placed correctly, assuming the reading error of the water wave arrival time $t_{ww} < 5$ ms; if the subsequent correlation of refracted waves as well as interface groups seems possible from trace to trace, we have an indication that the range uncertainties introduced in this case are small, since errors of the magnitude as discussed above will become evident immediately.

5

Sediment geoacoustics

Sediment core locations were selected with the aid of the seismic high-resolution profiles. Since we expected to encounter more consolidated sediments in depths of 3–5 m, we used a 4 m gravity corer. Eleven cores were collected with an average recovery depth of 3.80 m. Standard sedimentology analysis techniques were used to determine sediment grain size and porosity.

Sediments in the upper 4 m were clayey silts (Fig. 14) with sandy layers found below 4 m. Porosity in the upper layers ranged from 15% in the upper 20 cm to 55–60% near the clay/sand interface. Compressional wave velocity (Fig. 15) and attenuation and shear velocity in the cores were determined in the laboratory using a pulse technique (Richardson, 1986; Richardson et al., 1987). Examples of velocity profiles are shown in Figs. 16 and 17. In the upper layer (0–4 m) sediment compressional wave velocities c_p increase from 1470–1490 m/s. In the sandy layer below 4 m average velocities of $c_p = 1720$ m/s were measured. Shear-wave velocities ranged from $c_s = 17.7$–27.8 m/s in the silty-clay upper layer. No shear-wave velocities were measured in the lower sandy layer. A more detailed presentation of core data analysis as well as in situ measurements of shear properties will be forthcoming in other SACLANTCEN publications.

Results for shear-wave velocity of $c_s = 17.7$–27.8 m/s are well below those assumed and incorporated for the first simplified models (Snoek et al., 1986). Shear waves measured in the laboratory may be lower than in situ values as a result of the missing overload pressure of the water column (Richardson et al., 1989).

To correct shear-wave velocity gradients of core data collected in silts and clays for the overload pressure, Ohta and Goto (1978) give the following estimates $c_s = 78.93 \, D^{0.312}$ (D is the depth in this sediment). Applying these corrections to our core data we obtain obtain values of $c_s = 79$–121 m/s for the depth 1–4 m. Compensated for the overload, core data fit remarkable well with the shear-wave velocities obtained from correlation techniques described earlier.

Values incorporated were inferred from the interface velocities obtained under the assumption that shear-wave velocities on soft sediments follow the relation $c_{Scholte} \approx 0.9 c_s$ (see also Table 2).

CLAY

165-311

15-270

340

350

370

380

SAND

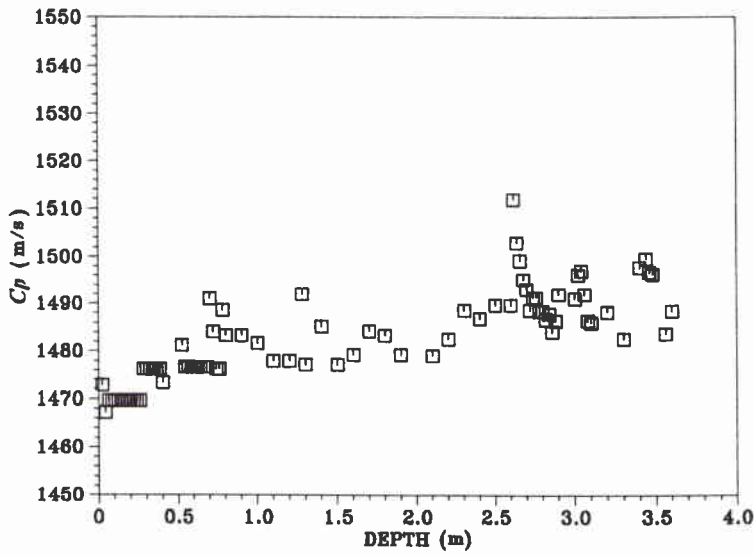Core depths in centimetres
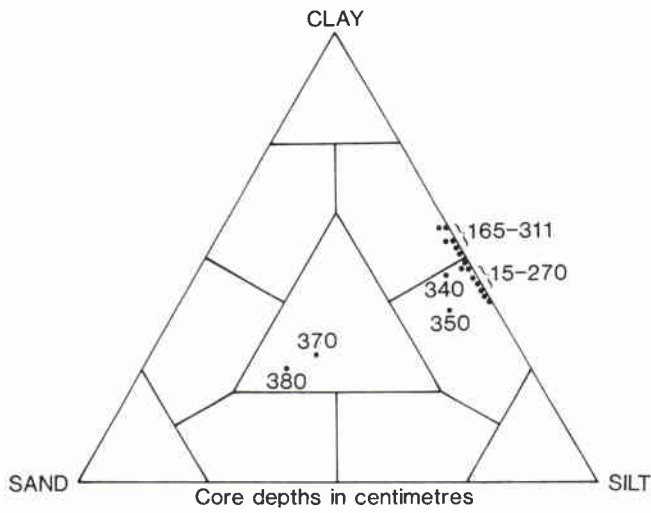
SILT

Figure 14 *Diagram for the silt, clay and sand distribution in core no. 195.*

Cp (m/s)
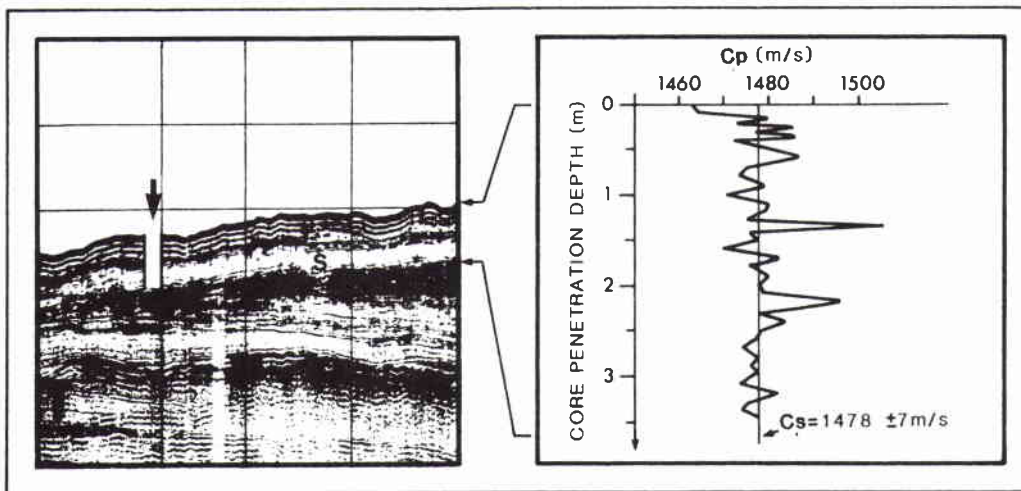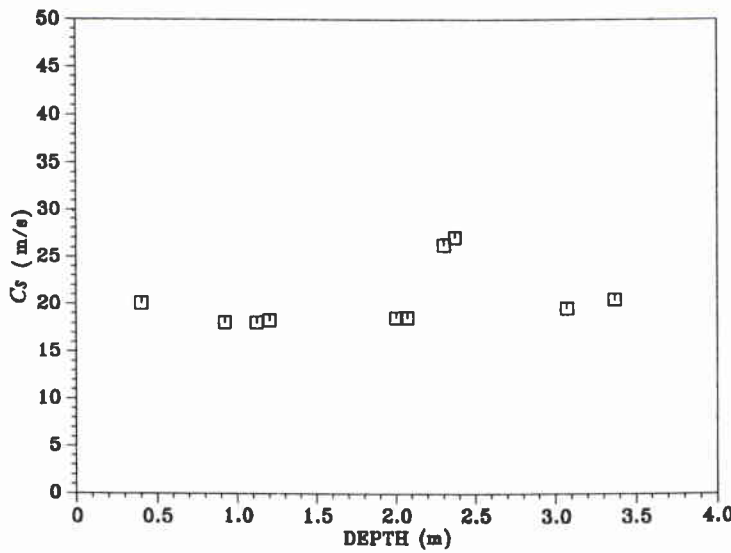
Figure 15 *Penetration of core at site of OBS array and interpretation.*

- 24 -

Figure 16 *Analysis of compressional velocities for core no. 191.*

Figure 17 *Analysis of shear velocities for core no. 191.*

6

Modelling

The fundamental problem involved with the inversion of geophysical data is given by the necessity to obtain initial parameters from observed data. The experimental methods described give us the two parameters c_p and $c_{Scholte}$. It has been shown (Jensen and Schmidt, 1986) that c_s can be inferred from $c_{Scholte}$. This is not sufficient to describe the propagation medium; what is further needed is the density and shear- and compresssional-wave attenuation. Core data will give us point measurements for the surficial sediments; information on deeper strata have to be deduced. Two different aproaches can be taken to model the data and thus 'parameterize' the seafloor; calculating the depth-dependent geoacoustical parameter, or solving the depth-separated wave equation by a numerical method. The Biot–Stoll model is based on the stress–strain behaviour of porous material and allows us to calculate the missing physical parameters by using parameter relationships. We, however, used the SACLANTCEN SAFARI code (Schmidt, 1988), a full wavefield technique developed to solve the wave equation in horizontal stratified media (Schmidt, 1983; 1984a,b). Here we decided to model the dispersion behaviour of the interface wavetrain instead of calculating synthetic seismograms and performing a wiggle-to-wiggle comparison.

This modelling approach was selected because the dispersive character of the propagating wave is directly related to the layering structure and hence to the property of the medium. Ideally both methods should converge for the correct input model. However, the complexity of the propagation media makes this task close to impossible to solve.

The procedure applied here was to calculate the dispersion characteristics (displayed as a Gabor matrix) of the real data, compute the dispersion curves for a given model using SAFARI, and try to match both data sets. We initially incorporated the very low values for the shear speed $v_s = 18$–28 m/s measured *in the laboratory* on the cores, which lead to a mismatch of measured and computed dispersion curves (Fig. 18). We then approached a solution iteratively (Fig. 19) and we ran the model with overload pressure corrected values, with $v_s = 79$–121 m/s. The input data for the best fit are given in Table 4.

However, it should be pointed out that there do exist some major problems in modelling a complex environment as presented here, since it is a gross simplification to treat this propagation area as a horizontally stratified fluid/solid range-independent environment. As a consequence, we have been able to match only the fundamen-

Table 4 *Input parameter for test site ocean bottom*

	Thickness H (m)	Wave speeds (m/s)		Attenuation (dB/λ)		Density ρ (g/cm^3)
		c_p	c_s	γ_p	γ_s	
Silt	4.0	1488	70–100	0.2	0.5	1.1
Sand	∞	1600	250	0.2	0.5	2.0

tal mode for this environment. However, the modelling approach provides the only means to obtain a physical idea of the environment and thus allows us to achieve a plausible interpretation of the measured data.
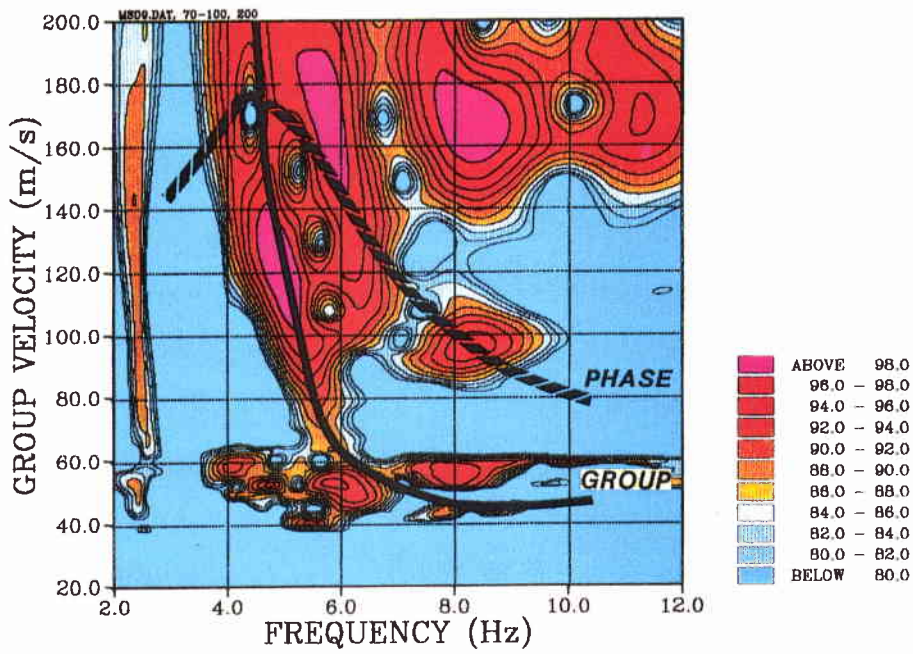
Figure 18 *Comparison of modelled (solid line) and computed dispersion curves based on uncorrected core velocities.*
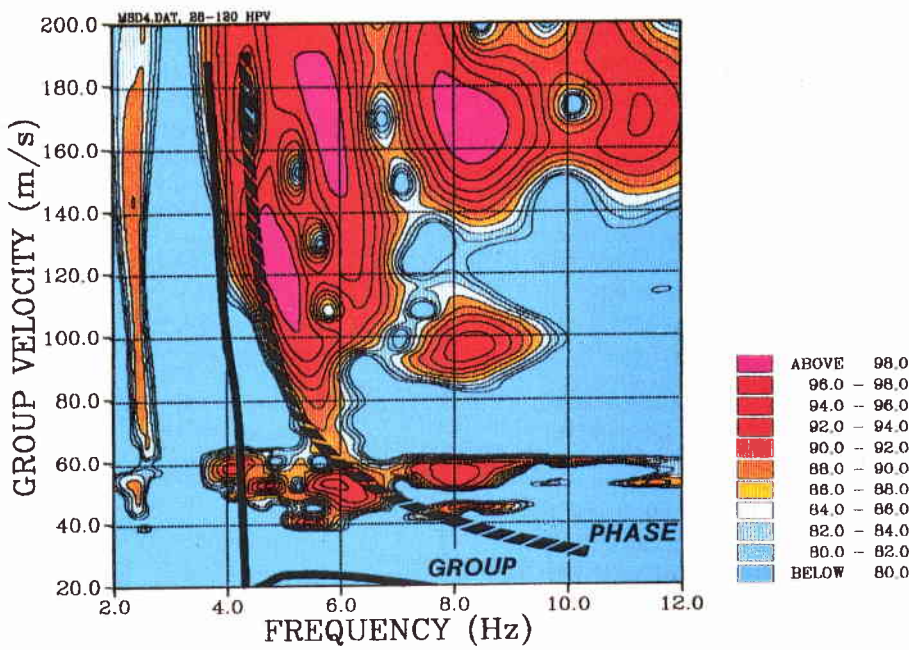
Figure 19 *Comparison of modelled (solid line) and computed dispersion curves, based on interface-wave analysis and corrected core velocities.*

7

Conclusion

Experimental results   In a linear system theory the transmission path of an acousti-cal signal generated in the water body or on the seafloor, transmitted to the seafloor, propagating through the sub-seafloor and finally arriving at the sensor placed on the seabottom, can be represented as a series of filters that modify the original signal considerably in amplitude and frequency. To be able to describe quantitatively the signal source from the analysis of the recorded signal, all parameters involved in the propagation should be known. Since under realistic field conditions this poses a problem impossible to solve, at least one has to come up with reasonable esti-mates. This means, one must try to understand the physics involved and try to solve the problems for those parameters we can control. It has been shown that the environmental conditions have a paramount impact on the generation and propaga-tion of seismic interface waves; i.e. the seismic response to an explosive source fired on the seafloor and recorded with an OBS reflects the complexity of the geological structures and facies conditions. We have been able to demonstrate that there is a notable *dependency* of interface wave propagation on the *azimuth* of the track. In confrontation with the high-resolution seismic profiles, however, it also becomes clear that we are talking of highly heterogeneous propagation media varying strongly in lateral as well as in vertical dimensions, interacting with the propagating inter-face wave. We encountered anomalous high attenuation of interface wave energy on one profile, possibly due to strong lateral inhomogeneities. Unfortunately, spatial coverage of the high-resolution seismics was too low to enable us to identify and outline the source of this attenuation. In view of the angular spacing of only 7° and the absence of these effects on the other profiles, the area of high attenuation can only be of limited extension.

The area selected can be considered as typical and representative for continental shelf areas with the propagation paths of seismic waves crossing complicated geo-logical structures. This in turn led to the fact that individual sources of interaction and conversion could not be discriminated sufficiently to establish generally valid statements.

The experiment has shown that a major effort is needed to advance from the quali-tative descriptions of *some*, to a quantitative formulation of *all* processes involved. Since data published so far do not permit an unequivocal formulation of all the problems, experiments have to be designed to understand and control the involved physics, e.g. to demonstrate the effects of different geoacoustical parameters on wave propagation.

Suggestions for future work   To start with this task asks for a laterally homogeneous area of well mapped and defined layers. Further basic requirements will be:

- Precise navigation and positioning aids, preferably a mini-ranger like system.

- Abundant information on the sub-seafloor structure with good spatial resolution.

- Geoacoustic information from cores representative for this region.

- Excitation sources of preferably different frequency content.

- Good spatial resolution of the energy distribution of the input signal in the water and/or in the seafloor and sub-seafloor.

- Extensive use of modelling.

The main goal of our work ultimately is to 'parameterize' the seafloor, i.e. to quantify the spatial variability of transmission and attenuation to allow a solid prediction for sound propagation. For the experimental part this also means that the common approach of investigating seismic waves in one site and acoustic propagation at another location, or at different times, has to be abandoned in favour of integrated measurements, i.e. the simultaneous measurement of the entire seismo-acoustic wavefield.

References

Akal, T., Barbagelata, A., Guidi, G. and Snoek, M. Time dependence of infrasonic ambient seafloor noise, *In*: Akal, T. and Berkson, J.M. *eds.* Ocean Seismo-Acoustics. New York, NY, Plenum, 1986: pp. 767–778.

Barbagelata, A., Michelozzi, E., Rauch, D., Schmalfeldt, B. Seismic sensing of extremely low-frequency sounds in coastal waters. *In*: INSTITUTE OF ELECTRICAL AND ELEC-TRONICS ENGINEERS. ACOUSTICS, SPEECH AND SIGNAL PROCESSING SOCI-ETY. ICASSP 82, proceedings of the IEEE international conference on acoustics, speech and signal processing, Paris, France, 3–5 May, 1982. Piscataway, NJ, IEEE, 1982: pp. 1878–1881.

Brocher, T.M., Iwatake, B.T. and Lindwall, D.A. Experimental studies of low-frequency waterborne and sedimentborne acoustic wave propagation on a continental shelf. *Journal of the Acoustical Society of America*, **74**, 1983: 960–972.

Bucker, H.P., Whitney, J.A. and Keir, D.L. Use of Stoneley waves to determine the shear velocity in ocean sediments. *Journal of the Acoustical Society*, **36**, 1964: 1595–1596.

Crampin, S., Jacob, A.W.B., Miller, A. and Neilson, G. The LOWNET radio-linked seismometer network in Scotland. *Geophysical Journal of the Royal Astronomical Society*, **21**, 1970: 207–216.

Damiani, V. Terrazzi marini e sollevamenti differenti fra i bacini del Lao e del Corvino, Calabria. *Bollettino, Società Geologica Italiana*, **89**, 1970: 145–158.

Davies, D. Dispersed Stoneley waves on the ocean bottom. *Bulletin of the Seismological Society of America*, **55**, 1965: 903–918.

Dziewonski, A.S., Bloch, S. and Landisman, M. A technique for the analysis of transient seismic signals. *Bulletin of the Seismological Society of America*, **59**, 1969: 427–444.

Essen, H.H., Janle, H., Schirmer, F. and Siebert, J. Propagation of surface waves in marine sediments. *Journal of Geophysics*, **49**, 1981: 115–122.

Finetti, I., Morelli, C. and Zarudski, E. Reflection seismic study of the Tyrrhenian Sea. *Bollettino di Geofisica Teorica ed Applicata*, **12**, 1970: 311–346.

Finetti, I. and Morelli, C. Geophysical exploration of the Mediterranean Sea. *Bollettino di Geofisica Teorica ed Applicata*, **15**, 1973: 263–340.

Ganley, D.C. and Kanasewich, E.R. Measurements of Absorption and Dispersion From Check Shot Surveys. *Journal of Geophysical Research*, **85**, 1980: 5219–5226.

Hamilton, E.L., Bucker, H.P., Keir, D.L. and Whitney, J.A. Velocities of compressional and shear waves in marine sediments determined in situ from a research submersible. *Journal of Geophysical Research*, **75**, 1970: 4039–4049.

Herron, E.M., Dorman, J. and Drake, C.L. Seismic study of the sediments in the Hudson River. *Journal of Geophysical Research*, **73**, 1968: 4701–4709.

Holt, R.M., Hovem, J.M. and Syrstad, J. Shear modulus profiling of near bottom sediments using boundary waves. *In*: Pace, N.G. *ed.* Acoustics and the Sea-bed. Bath, UK, Bath University Press, 1983: 317–325.

Jensen, F.B. and Schmidt, H. Shear properties of ocean sediments determined from numerical modelling of Scholte wave data. *In*: Akal, T. and Berkson, J.M., *eds*. Ocean Seismo-Acoustics. New York, NY, Plenum, 1986: pp. 683–692.

MacBeth, C.D. and Burton, P.W. Surface waves generated by underwater explosions offshore Scotland. *Geophysical Journal of the Royal Astronomical Society*, **94**, 1988: 285–294.

McDaniel, S.T. and Beebe, J.H. Influence of semiconsolidated sediments on sound propagation in a coastal region. *In*: Kuperman, W.A. and Jensen, F.B. *eds*. Bottom-Interacting Ocean Acoustics. New York, NY, Plenum, 1980: pp. 493–505.

Möller, L. Seismische Untersuchungen in Sedimenten der Nordsee. Ph.D. thesis, Hamburg University, Germany, 1983.

Ohta, Y. and Goto, N. Empirical shear wave velocity equations in terms of characteristic soil indexes. *Earthquake Engineering and Structural Dynamics*, **6**, 1978: 167–187.

Phinney, R.A. Propagation of Leaking Interface Waves. *Bulletin of the Seismological Society of America*, **51**, 1961: 527–555.

Rauch, D. Seismic Interface waves in coastal waters: a review, SACLANTCEN SR-42. La Spezia, Italy, SACLANT ASW Research Centre, 1980. [AD A 095 018]

Rauch, D. On the role of bottom interface waves in ocean seismo-acoustics: a review. *In*: Akal, T. and Berkson, J.M., *eds*. Ocean Seismo-Acoustics. New York, NY, Plenum, 1986: pp. 623–641.

Richardson, M.D. Spatial variability of surficial shallow-water sediment geoacoustic properties. *In*: Akal, T. and Berkson, J.M. *eds*. Ocean Seismo-Acoustics. New York, NY, Plenum, 1986: pp. 527–536.

Richardson, M.D., Curzi, P.V., Muzi, E., Miaschi, B. and Barbagelata, A. Measurements of shear wave velocity in marine sediments. *In*: Lara-Saenz, A., Ranz-Guerra, C. and Carbo-Fite, C. *eds*. Acoustics and Ocean Bottom, II FASE Specialized Conference. Madrid, Spain, Consejo Superior de Investigaciones Cientificas, 1987: pp. 75–84.

Richardson, M.D., Muzi, E., Troiano, L. and Miaschi, B. Sediment shear waves: A comparison of *in situ* and laboratory measurements. SACLANTCEN SM-210. La Spezia, Italy, SACLANT Undersea Research Centre, 1989.

Sauter, A.W., Dorman, L.M. and Schreiner, A.E. A study of seafloor structure using ocean bottom shots and receivers. *In*: Akal, T. and Berkson, J.M. *eds*. Ocean Seismo-Acoustics. New York, NY, Plenum, 1986: pp. 673–681.

Schirmer, F. Experimental determination of properties of the Scholte wave in the ocean bottom at the North Sea. *In*: Kuperman, W.A. and Jensen, F.B. *eds*. Bottom-Interacting Ocean Acoustics, New York, NY, Plenum, 1980: pp. 285–298.

Schmalfeldt, B. and Rauch, D. Explosion-generated seismic interface waves in shallow water: experimental results, SACLANTCEN SR-71. La Spezia, Italy, SACLANT ASW Research Centre, 1983. [AD A 134 551]

Schmalfeldt, B. and Ali, H.B. Low-frequency seismic and hydroacoustic studies in the Oslofjord and the Kattegat, SACLANTCEN SM-193. La Spezia, Italy, SACLANT ASW Research Centre, 1987. [AD C 955 545]

Schmidt, H. SAFARI, Seismo-Acoustic Fast field Algorithm for Range Independent environments: Users guide, SACLANTCEN SR-113. La Spezia, Italy, SACLANT Undersea Research Centre, 1988. [AD A 200 581]

Schmidt, H. Excitation and propagation of interface waves in a stratified sea-bed. *In*: Pace, N.G. *ed.* Acoustics and the Sea-Bed. Bath, UK, Bath University Press, 1983: pp. 327–334.

Schmidt, H. Numerical modelling of seismic interface waves, SACLANTCEN SM-169. La Spezia, Italy, SACLANT Undersea Research Centre, 1984a. [AD A 137 250]

Schmidt, H. Modelling of pulse propagation in layered media using a new Fast Field Program. *In*: Felsen, L.B. *ed.* Hybrid Formulation of Wave Propagation and Scattering. Dordrecht, The Netherlands, Nijhoff, 1984b: pp. 337–356.

Selli, R. An outline of the Italian Messinian. *In*: Drooger, C.W., *ed.* Messinian Events in the Mediterranean. Amsterdam, North Holland, 1973: pp. 150–171.

Snoek, M., Guidi, G. and Michelozzi, E. Interface wave studies on the Ligurian shelf using an OBS array: Experimental results and propagation models. *In*: Akal, T. and Berkson, J.M. *eds.* Ocean Seismo-Acoustics. New York, NY, Plenum, 1986: pp. 663–672.

Snoek, M. and Rauch, D. Anisotropic behaviour of Interface wave propagation for near surface sediments. *In*: Lara-Saenz, A., Ranz-Guerra, C. and Carbo-Fite, C. *eds.* Acoustics and Ocean Bottom, II FASE Specialized Conference. Madrid, Spain, Consejo Superior de Investigaciones Cientificas, 1987: pp. 201–209.

Snoek, M., Böttcher, C. and Schneider, W. DFG: OBSCAL Report. Ocean bottom seismometer intercalibration and coupling experiment, test outlines and events. Hamburg, Institut für Geophysik, 1982.

Snoek, M. and Herber, R. Qualitative aspects of seismograph/ocean bottom interaction. SACLANTCEN SM-206. La Spezia, Italy, SACLANT Undersea Research Centre, 1987. [AD A 198 652]

Staal, P.H. and Chapman, D.M.F. Observations of Interface waves and low-frequency acoustic propagation over a rough granite seabed. *In*: Akal, T. and Berkson, J.M. *eds.* Ocean Seismo-Acoustics. New York, NY, Plenum, 1986: pp. 643–652.

Stangerup, P. A detailed study of sound reflections from a layered ocean bottom, SACLANTCEN TR-42. La Spezia, Italy, SACLANT ASW Research Centre, 1965. [AD 466 138]

Stoll, R.D., Bryan, G.M., Flood, R., Chayes, D. and Manley, P. Shallow seismic experiments using shear waves. *Journal of the Acoustical Society of America*, **83**, 1988: 93–102.

Sutton, G.H., Duennebier, F.K. and Iwatake, B. Coupling of ocean bottom seismometers to soft bottom. *Marine Geophysical Researches*, **5**, 1981a: 35–51.

Sutton, G.H., Duennebier, F.K., Iwatake, B., Tuthill, J.D., Lewis, B.T.R. and Ewing, J. An overview and general results of the Lopez Island OBS experiment. *Marine Geophysical Researches*, **5**, 1981b: 3–34.

Sutton, G.H. and Duennebier, F.K. Optimum design of ocean bottom seismometers. *Marine Geophysical Researches*, **9**, 1988: 47–65.

Trehu, A.M. Coupling of ocean bottom seismometers to sediments: results of tests with the US Geological Survey ocean bottom seismometer. *Bulletin of the Seismological Society of America*, **75**, 1985: 271–289.

Tuthill, J.D., Lewis, B.R. and Garmany, J.D. Stoneley waves, Lopez Island noise, and deep sea noise from 1 to 5 Hz. *Marine Geophysical Researches*, **5**, 1981: 95–108.

Whitmarsh, R.B. and Lilwall, R.C. A new method for determination of in-situ shear-wave velocity in deep-sea sediments. *Geophysics*, **47**, 1982: 1745.

Initial Distribution for SM-229

Ministries of Defence

JSPHQ Belgium	2
DND Canada	10
CHOD Denmark	8
MOD France	8
MOD Germany	15
MOD Greece	11
MOD Italy	10
MOD Netherlands	12
CHOD Norway	10
MOD Portugal	5
MOD Spain	2
MOD Turkey	5
MOD UK	20
SECDEF US	60

NATO Authorities

Defence Planning Committee	3
NAMILCOM	2
SACLANT	3
CINCIBERLANT	1

SCNR for SACLANTCEN

SCNR Belgium	1
SCNR Canada	1
SCNR Denmark	1
SCNR Germany	1
SCNR Greece	1
SCNR Italy	1
SCNR Netherlands	1
SCNR Norway	1
SCNR Portugal	1
SCNR Spain	1
SCNR Turkey	1
SCNR UK	1
SCNR US	2
SECGEN Rep. SCNR	1
NAMILCOM Rep. SCNR	1

National Liaison Officers

NLO Canada	1
NLO Denmark	1
NLO Germany	1
NLO Italy	1
NLO Netherlands	1
NLO UK	1
NLO US	1

NLR to SACLANT

NLR Belgium	1
NLR Canada	1
NLR Denmark	1
NLR Germany	1
NLR Greece	1
NLR Italy	1
NLR Netherlands	1
NLR Norway	1
NLR Portugal	1
NLR Turkey	1
NLR UK	1

Total external distribution	221
SACLANTCEN Library	10
Stock	29
Total number of copies	260